physical sciences forum

MDPI

Proceeding Paper

Coherent Neutrino Scattering and Quenching Factor Measurement †

Jiajun Liao

School of Physics, Sun Yat-sen University, Guangzhou 510275, China; liaojiajun@mail.sysu.edu.cn

† Presented at the 23rd International Workshop on Neutrinos from Accelerators, Salt Lake City, UT, USA, 30–31 July 2022.

Abstract: The latest direct measurements of the germanium quenching factor deviate significantly from the standard Lindhard model for nuclear recoil energies at the sub keV region. Here, we show that the recently measured coherent elastic neutrino–nucleus scattering (CEνNS) data from reactor antineutrinos can be used to probe the quenching factor model, and a 2σ improvement can be achieved in the fit to the measured CEνNS data if the quenching factor is described by a modified Lindhard model with a negative value of q, which is also consistent with the direct quenching factor measurement. Constraints on the parameter space of a light vector or scalar mediator that couples to neutrinos and quarks, and on a neutrino magnetic moment, are also placed by using the measured CEνNS data, and we find that they are quite sensitive to the quenching factor model at low recoil energies.

Keywords: CEνNS; quenching factor; light mediator

1. Introduction

The study of nuclear recoils plays an important role in both dark matter direct detection experiments and Coherent elastic neutrino–nucleus scattering (CEνNS) experiments. CEνNS is a process in which low-energy neutrinos scatter off a nucleus as an entire entity via neutral current interactions [1]. This process was first observed by the COHERENT collaboration [2] by using a pion-decay-at-rest (πDAR) neutrino source with a cesium-iodide detector. The COHERENT collaboration also confirmed the existence of CEνNS with an argon detector at a confidence level (CL) of more than 3σ using the same source [3]. The observation of CEνNS opens a new window to probe neutrino and nuclear physics at low energies; for a recent review, see Ref. [4] and references therein.

Due to the abundant neutrino fluxes produced by nuclear power reactors, reactor antineutrinos also serve as an ideal source for the measurement of CEνNS. However, the observation of CEνNS from reactor antineutrinos is much more difficult than from the πDAR source due to the lower energies of reactor antineutrinos. Thus, a detector with a very low threshold is required to detect CEνNS from reactor antineutrinos. Currently, CONNIE [5] and CONUS [6] experiments have placed constraints on CEνNS with reactor antineutrinos with a silicon and germanium detector, respectively. Colaresi et al. have also used a germanium detector to measure CEνNS at the Dresden-II power reactor [7], and they found the first hint of CEνNS from reactor antineutrinos in a recent measurement made with the NCC-1701 germanium detector [8]. In addition, the latest direct measurements of the germanium quenching factor show a significant deviation from the standard Lindhard model for nuclear recoil energies in the sub keV region [9]. In this work, we use the recently measured CEνNS spectrum to probe the germanium quenching factor model.

check for updates

Citation: Liao, J. Coherent Neutrino Scattering and Quenching Factor Measurement †. *Phys. Sci. Forum* **2023**, *8*, 18. https://doi.org/10.3390/psf2023008018

Academic Editor: Yue Zhao

Published: 21 July 2023

2. CEνNS

Here we show the calculation of the CEνNS spectrum from reactor antineutrinos in details. The differential CEνNS event rate with respect to the nuclear recoil energy E_R is given by

$$\frac{dR}{dE_R} = N_T \int \frac{d\Phi}{dE_\nu} \frac{d\sigma}{dE_R} dE_\nu \,, \tag{1}$$

where N_T is the number of nuclei in the detector, and $\frac{d\Phi}{dE_\nu}$ is the reactor antineutrino flux. The differential CEνNS cross section in the standard model (SM) is given by [1]

$$\frac{d\sigma_{SM}}{dE_R} = \frac{G_F^2 M}{4\pi} q_W^2 \left(1 - \frac{M E_R}{2E_\nu^2}\right) F^2(\mathfrak{q}) \,, \tag{2}$$

where M is the nuclear mass, G_F is the Fermi coupling constant, $q_W = N - (1 - 4\sin^2\theta_W)Z$ with θ_W the weak mixing angle, and $F(\mathfrak{q})$ is the Klein–Nystrand form factor [10]. Due to the low momentum transfer in CEνNS with reactor antineutrinos, the calculated signal is not sensitive to the specific choice of the form factors and its uncertainties [11].

The measured CEνNS spectrum is strongly dependent on the germanium quenching factor Q, which is defined as the ratio of the observable ionization energy E_I to the nuclear recoil energy E_R, i.e., $Q \equiv E_I/E_R$. Therefore, the differential event rate with respect to E_I is

$$\frac{dR}{dE_I} = \frac{dR}{dE_R}\left(\frac{1}{Q} - \frac{E_I}{Q^2}\frac{dQ}{dE_I}\right). \tag{3}$$

Currently, experimental measurements of the quenching factor are well described by the standard Lindhard model [12] for $E_R \gtrsim 1\ \mathrm{keV_{nr}}$, which can be clearly seen from Figure 3 in Appendix II of Ref. [13]. In the Lindhard model, the quenching factor is given by

$$Q(E_R) = \frac{k\, g(\epsilon)}{1 + k\, g(\epsilon)} \,, \tag{4}$$

where $g(\epsilon)$ is well fitted by $g(\epsilon) = 3\,\epsilon^{0.15} + 0.7\,\epsilon^{0.6} + \epsilon$ with $\epsilon = 11.5\, Z^{-\frac{7}{3}} \left(\frac{E_R}{\mathrm{keV}}\right)$ [14], and $k = 0.133 Z^{\frac{2}{3}} A^{-\frac{1}{2}} = 0.157$ for germanium in the standard Lindhard model.

However, for sub-keV nuclear recoils, the quenching factors are not well modeled by the Lindhard model due to uncertainties in nuclear scattering and stopping at low energies [15,16]. A recent measurement of the germanium quenching factor shows a departure from the Lindhard model for nuclear recoil energies below $\sim$1 $\mathrm{keV_{nr}}$ [9], and the overall shape of the quenching factor can be parameterized by a modified Lindhard model [16,17],

$$Q(E_R) = \frac{k\, g(\epsilon)}{1 + k\, g(\epsilon)} - \frac{q}{\epsilon} \,, \tag{5}$$

where the parameter q can be negative (positive) if the energy given to electrons is enhanced (cutoff). After taking into account of the energy resolution, the differential event rate with respect to the measured energy E_M is

$$\frac{dR}{dE_M} = \frac{\int_0^\infty G(E_M, E_I, \sigma^2) \frac{dR}{dE_I} dE_I}{\int_0^\infty G(E_M, E_I, \sigma^2) dE_I} \,. \tag{6}$$

where

$$G(E_M, E_I, \sigma^2) = \frac{1}{\sqrt{2\pi\sigma^2}} \exp\left[-\frac{(E_M - E_I)^2}{2\sigma^2}\right] , \tag{7}$$

and $\sigma^2 = \sigma_n^2 + E_I \eta F$ with $\sigma_n = 68.5$ eV the intrinsic electronic noise, $\eta = 2.96$ eV the average energy to produce an electron–hole pair in germanium, and $F \approx 0.105$ the Fano factor taken from Ref. [8].

3. Results and Discussion

We first use the measured CEνNS data [8] to probe the quenching factor model. The CEνNS data are measured by a low-noise 3 kg germanium detector with a distance of $\sim$10 m from the 2.96 GW Dresden-II power reactor for a 96.4 day exposure. We analyze the spectrum of residual counts in Figure 5 of Ref. [8] and fit 20 bins in E_M from 0.2 to 0.4 keV$_{\rm ee}$. We use the following χ^2 to evaluate the statistical significance of a theoretical model, i.e.,

$$\chi^2 = \sum_i \left[\frac{N^i_{\rm exp} - N^i_{\rm th}(1+\alpha)}{\sigma_i} \right]^2 + \left(\frac{\alpha}{\sigma_\alpha} \right)^2, \tag{8}$$

where $N^i_{\rm exp}$ ($N^i_{\rm th}$) is the measured (predicted) number of residual counts per bin and σ_i is the corresponding uncertainty with $\sigma_\alpha = 5\%$ being the percent uncertainty in the reactor neutrino flux normalization. The minimum of χ^2 is obtained by marginalizing over the auxiliary parameter α. We get $\chi^2_{\rm min} = 14.3$ for the SM with the standard Lindhard model for the quenching factor. Moreover, we find that a modified Lindhard model can improves the fit. In order to be compatible with quenching factor measurements at high recoil energies [13], we only consider k values in the range of [0.147, 0.167]. The 1σ, 90% CL, and 2σ allowed regions in the (k, q) space are shown in Figure 1. The best-fit point is located at $k = 0.167$ and $q = -22.2 \times 10^{-5}$, with $\chi^2_{\rm min} = 8.14$. We can see that it is a substantial improvement over the standard Lindhard model. Furthermore, we notice that this best-fit point is consistent with the direct quenching factor measurements of Ref. [9], which can be parametrized by a negative q, as shown in Ref. [17]. Hence, the measured NCC-1701 data provide an independent probe of the quenching factor. From the left panel of Figure 1, we see that the data are not sensitive to k, and negative values of q are preferred. We also plot $\Delta\chi^2 \equiv \chi^2(q) - \chi^2_{\rm min}$ for $k = 0.157$ in the right panel of Figure 1. We can see that the measured data prefer $q < 0$ at 2.5σ CL.

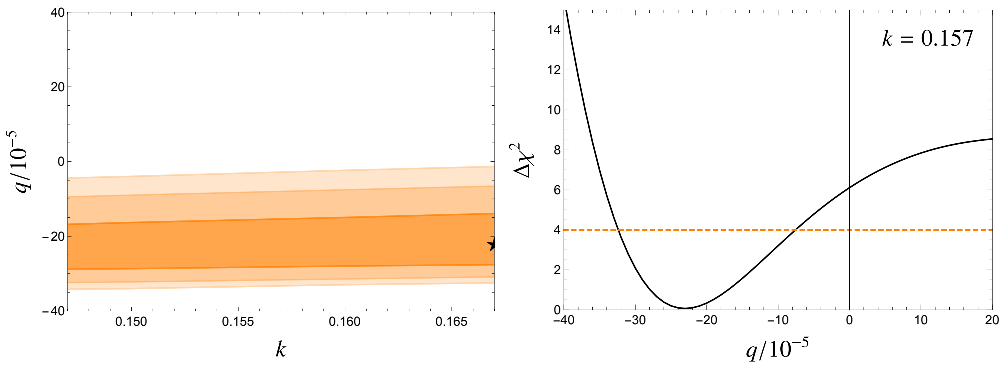

Figure 1. Left panel: The 1σ, 90% CL, and 2σ allowed regions in the (k, q) plane for the modified quenching factor model. The best fit point is marked by a star. Right panel: $\Delta\chi^2 \equiv \chi^2(q) - \chi^2_{\rm min}$ for a fixed $k = 0.157$ [18].

We also use the measured CEνNS spectrum to place constraints on three simple new physics scenarios in the neutrino sector: a light Z' or scalar that couples to neutrinos and quarks universally, and a large neutrino magnetic moment. The differential cross sections of the three new physics scenarios are given in Ref. [18], and we use the same χ^2 in Equation (8) for our analysis. In order to place constraints on the new physics parameter space, we scan over possible values of the coupling and mediator mass for the light Z' and scalar cases. We also consider two different treatments of the quenching factor: (i) we fix the quenching factor as the standard Lindhard model, and (ii) we reduce the dependence on the quenching factor model by marginalizing over k and q in the modified Lindhard model. The best fit points and χ^2_{min}/dof values are listed in Table 1. We see that if the standard Lindhard model is assumed for the quenching factor, the data show a mild preference for the new physics scenarios compared to the SM. Furthermore, we find that the constraints are qualitatively affected by the quenching factor model due to its dependence on q [18]. The best-fit value of the neutrino magnetic moment, and the corresponding χ^2_{min}, are also provided in Table 1. We find that the 90% CL bound from NCC-1701 data is $\mu_\nu < 4.0 \times 10^{-10}\mu_B$, which is an order of magnitude weaker than the current bound on the electron neutrino magnetic moment by the GEMMA experiment, $\mu_\nu < 2.9 \times 10^{-11}\mu_B$ [19].

Table 1. Values of χ^2_{min}/dof for the SM and new physics scenarios with various quenching factor model from the NCC-1701 data.

Scenarios	k	$q/10^{-5}$	χ^2_{min}/**dof**
SM w/standard Lindhard	0.157	0	14.34/19
SM w/modifed Lindhard w/fixed k	0.157	−23.8	8.28/18
SM w/modified Lindhard w/$0.147 \le k \le 0.167$	0.167	−22.2	8.14/17
light Z' w/$m_{Z'} = 63.1$ MeV, $g_{Z'} = 1.4 \times 10^{-4}$	0.157	0	9.09/17
light scalar w/$m_\phi = 25.1$ MeV, $g_\phi = 1.6 \times 10^{-5}$	0.157	0	7.77/17
neutrino magnetic moment w/$\mu_\nu = 2.5 \times 10^{-10}\mu_B$	0.157	0	11.71/18

4. Conclusions

Recent direct measurement of germanium quenching factor indicates a departure from the standard Lindhard model at low energies, and this deviation can be parameterized by a negative q in the modified Lindhard model. The recently measured CEνNS data can be also used to provide an independent probe of the quenching factor models. We show that the latest measured NCC-1701 data prefer negative values of q in the modified Lindhard model, and the best-fit point is consistent with the direct quenching factor measurements. A precise measurement of the quenching factor is essential to detect new physics at CEνNS. If the germanium quenching factor is described by the standard Lindhard model correctly, then the NCC-1701 data may indicate the presence of a light vector or scalar or a large neutrino magnetic moment.

Funding: This research was funded by the National Natural Science Foundation of China, grant number 12275368.

Institutional Review Board Statement: Not applicable.

Informed Consent Statement: Not applicable.

Data Availability Statement: Not applicable.

Conflicts of Interest: The author declares no conflict of interest.

References

1. Freedman, D.Z. Coherent neutrino nucleus scattering as a probe of the weak neutral current. *Phys. Rev. D* **1974**, *9*, 1389. [CrossRef]
2. Akimov, D.; Albert, J.B.; An P.; Awe, C.; Barbeau, P.S.; Becker, B.; Belov, V.; Brown, A.; Bolozdynya, A.; Cabrera-Palmer, B.; et al. Observation of coherent elastic neutrino-nucleus scattering. *Science* **2017**, *357*, 1123–1126. [CrossRef] [PubMed]
3. Akimov, D.; Albert, J.B.; An P.; Awe, C.; Barbeau, P.S.; Becker, B.; Belov, V.; Bernardi, I.; Blackston, M.A.; Blokl, L.; et al. First Measurement of Coherent Elastic Neutrino-Nucleus Scattering on Argon. *Phys. Rev. Lett.* **2021**, *126*, 012002. [CrossRef] [PubMed]
4. Papoulias, D.K.; Kosmas, T.S.; Kuno, Y. Recent probes of standard and non-standard neutrino physics with nuclei. *Front. Phys.* **2019**, *7*, 191. [CrossRef]
5. Aguilar-Arevalo, A.; Bertou, X.; Bonifazi, C.; Cancelo, G.; Castañeda, A.; Vergara, B.C.; Chavez, C.; D'Olivo, J.C.; Dos Anjos, J.C.; Estrada, J.; et al. Exploring low-energy neutrino physics with the Coherent Neutrino Nucleus Interaction Experiment. *Phys. Rev. D* **2019**, *100*, 092005. [CrossRef]

6. Bonet, H.; Bonhomme, A.; Buck, C.; Fülber, K.; Hakenmüller, J.; Heusser, G.; Hugle, T.; Lindner, M.; Maneschg, W.; Rink, T.; et al. Constraints on Elastic Neutrino Nucleus Scattering in the Fully Coherent Regime from the CONUS Experiment. *Phys. Rev. Lett.* **2021**, *126*, 041804. [CrossRef] [PubMed]
7. Colaresi, J.; Collar, J.I.; Hossbach, T.W.; Kavner, A.R.L.; Lewis, C.M.; Robinson, A.E.; Yocum, K.M. First results from a search for coherent elastic neutrino-nucleus scattering at a reactor site. *Phys. Rev. D* **2021**, *104*, 072003. [CrossRef]
8. Colaresi, J.; Collar, J.I.; Hossbach, T.W.; Lewis, C.M.; Yocum, K.M. Suggestive evidence for coherent elastic neutrino-nucleus scattering from reactor antineutrinos. *arXiv* **2022**. arXiv:2202.09672.
9. Collar, J.I.; Kavner, A.R.L.; Lewis, C.M. Germanium response to sub-keV nuclear recoils: A multipronged experimental characterization. *Phys. Rev. D* **2021**, *103*, 122003. [CrossRef]
10. Klein, S.R.; Nystrand, J. Interference in exclusive vector meson production in heavy ion collisions. *Phys. Rev. Lett.* **2000**, *84*, 2330–2333. [CrossRef]
11. Sierra, D.A.; Liao, J.; Marfatia, D. Impact of form factor uncertainties on interpretations of coherent elastic neutrino-nucleus scattering data. *J. High Energy Phys.* **2019**, *6*, 141. [CrossRef]
12. Lindhard, J.; Nielsen, V.; Scharff, M.; Thomsen, P. Integral equations governing radiation effects. *Kgl. Danske Videnskab. Selskab. Mat. Fys. Medd.* **1963**, *33*, 10.
13. Lin, S.T.; Li, H.B.; Li, X.; Lin, S.K.; Wong, H.T.; Deniz, M.; Fang, B.B.; He, D.; Li, J.; Lin, C.W.; et al. New limits on spin-independent and spin-dependent couplings of low-mass WIMP dark matter with a germanium detector at a threshold of 220 eV. *Phys. Rev. D* **2009**, *79*, 061101. [CrossRef]
14. Lewin, J.D.; Smith, P.F. Review of mathematics, numerical factors, and corrections for dark matter experiments based on elastic nuclear recoil. *Astropart. Phys.* **1996**, *6*, 87–112. [CrossRef]
15. Lindhard, J.; Scharff, M.; Schiott, H.E. Range concepts and heavy ion ranges. *Mat. Fys. Medd. Dan. Vid. Selsk.* **1963**, *33*, 14.
16. Sorensen, P. Atomic limits in the search for galactic dark matter. *Phys. Rev. D* **2015**, *91*, 083509. [CrossRef]
17. Liao, J.; Liu, H.; Marfatia, D. Coherent neutrino scattering and the Migdal effect on the quenching factor. *Phys. Rev. D* **2021**, *104*, 015005. [CrossRef]
18. Liao, J.; Liu, H.; Marfatia, D. Implications of the first evidence for coherent elastic scattering of reactor neutrinos. *Phys. Rev. D* **2022**, *106*, L031702. [CrossRef]
19. Beda, A.; Brudanin, V.; Egorov, V.; Medvedev, D.; Pogosov, V.; Shirchenko, M.; Starostin, A. The results of search for the neutrino magnetic moment in GEMMA experiment. *Adv. High Energy Phys.* **2012**, *2012*, 350150. [CrossRef]